Synthesis, characterization, optical, thermal and electrical properties of polybenzimidazoles

Article *in* Journal of Macromolecular Science Part A Pure and Applied Chemistry · January 2018

DOI: 10.1080/10601325.2018.1424550

CITATIONS
17

READS
645

4 authors:

Siddeswaran Anand
K S R Institute for Engineering and Technology
16 PUBLICATIONS **154** CITATIONS
SEE PROFILE

Athianna Muthusamy
Sri Ramakrishna Mission Vidyalaya College of Arts and Science
53 PUBLICATIONS **508** CITATIONS
SEE PROFILE

Dineshkumar Sengottuvelu
University of Mississippi
30 PUBLICATIONS **306** CITATIONS
SEE PROFILE

Nagarajan Kannapiran
Sri Ramakrishna Mission vidyalaya college of Arts and Science, Coimbatore
15 PUBLICATIONS **142** CITATIONS
SEE PROFILE

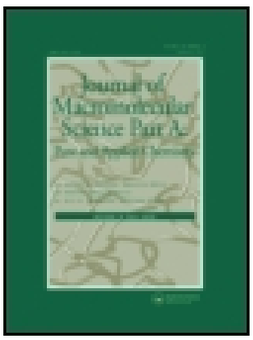

Taylor & Francis
Taylor & Francis Group

Journal of Macromolecular Science, Part A
Pure and Applied Chemistry

ISSN: 1060-1325 (Print) 1520-5738 (Online) Journal homepage: http://www.tandfonline.com/loi/lmsa20

Synthesis, characterization, optical, thermal and electrical properties of polybenzimidazoles

Siddeswaran Anand, Athianna Muthusamy, Sengottuvelu Dineshkumar & Nagarajan Kannapiran

To cite this article: Siddeswaran Anand, Athianna Muthusamy, Sengottuvelu Dineshkumar & Nagarajan Kannapiran (2018): Synthesis, characterization, optical, thermal and electrical properties of polybenzimidazoles, Journal of Macromolecular Science, Part A, DOI: 10.1080/10601325.2018.1424550

To link to this article: https://doi.org/10.1080/10601325.2018.1424550

JOURNAL OF MACROMOLECULAR SCIENCE, PART A: PURE AND APPLIED CHEMISTRY
2018, VOL. 0, NO. 0, 1–10
https://doi.org/10.1080/10601325.2018.1424550

Synthesis, characterization, optical, thermal and electrical properties of polybenzimidazoles

Siddeswaran Anand[a], Athianna Muthusamy[a], Sengottuvelu Dineshkumar[b] and Nagarajan Kannapiran[a]

[a]PG and Research Department of Chemistry, Sri Ramakrishna Mission Vidyalaya College of Arts and Science, Coimbatore, Tamil Nadu, India; [b]Department of Chemistry, Birla Institute of Technology and Science, Pilani Campus, Pilani, Rajasthan, India

ABSTRACT

The variation of dielectric constant and dielectric loss of two novel polybenzimidazole (PBI) were studied at constant temperature with variable frequency. The polymers have shown maximum dielectric constant at low applied frequency 50 Hz at 393 K due to the space charge polarization. The AC conductivity and activation energy of polymers were arrived from dielectric constant and dielectric loss values. PBIs were synthesized by the oxidative polycondensation of benzimidazole monomers, 2-(1H-benzo [d] imidazole-2-yl)-4-bromophenol (BIBP), and 2-(1H-benzo [d] imidazole-2-yl)-6-methoxyphenol (BIMP) in an aqueous alkaline medium using NaOCl as oxidant. The monomers and polymers were characterized by various spectroscopic techniques. Fluorescence spectra of monomers and polymers showed their λ_{max} emission in the region of 472–479 and 463–472 nm respectively. The electrical conductivities of iodine doped polybenzimidazoles were measured by four-point probe technique and it increases with increase in iodine vapour contact time. The electrical conductivity values were correlated with the charge density on imidazole nitrogen obtained from Huckel calculation method. Both the PBI are having reasonably good thermal stability and are shown by high carbines residues of around 40% at 500°C in thermogravimetric analysis.

ARTICLE HISTORY
Received May 2017
Revised October 2017
Accepted January 2018

KEYWORDS
Polybenzimidazoles; Electrical conductivity; Dielectric properties; AC conductivity

1. Introduction

Dielectric polymers have attracted the attention of researchers, because of their easy of processing, allowing them into flexible forms, high breakdown strength, high energy density, high reactivity, light weight and low cost.[1,2] Polymer dielectrics have several advantages over nonpolymeric dielectric materials due to their high dielectric constant, low dielectric loss, low operating voltage, good efficiency, low moisture absorbent, chemical inertness, high mechanical property and good thermal conductivity.[3–8] These low cost polymer dielectrics are widely used in electrical insulation, power circuit boards, electronic packaging, and excellent chemical resistance.[9] Polymers have been considered as one of the potential materials for dielectrics. Because of its high dielectric breakdown strength, low dielectric loss and environmental stability. So it can be used for preparing embedded micro capacitors to meet the requirement of miniaturization trend of integrated circuits.[10] In the recent years some work has been focused on high dielectric constant of conjugated polymers such as polypyrrole, polythiophene, poly (vinylidene fluoride), epoxy, polyimide and polystyrene. These high dielectric constants of conjugated polymers are mainly used in microelectronics, aerospace and sustainable energy technologies.[11–15] Polybenzimidazoles have electrical conductivity at high temperature range, high heat resistance, and mechanical property, film forming ability, good solubility, and high thermal and oxidative stability. These distinctive are appropriate for the construct of dielectric material for high energy storage device applications.[16–18] Moreover, PBI possesses the both proton acceptor (−N =) and donor (−NH) hydrogen bonding sites that exhibit specific interaction with polar solvents[19,20] and it is having free charge separation in the excited state results the development to response dielectric properties.

In this work, we have synthesized two PBIs through oxidative polycondensation of benzimidazole monomers using NaOCl as an oxidant. The structure of the synthesized compounds was confirmed by FT- IR, UV-visible and NMR spectroscopic techniques. The dielectric properties of synthesized polymers at different temperature and frequency were carried out. AC conductivity and activation energy of polymers were evaluated. The fluorescence study of benzimidazole monomers and PBIs were carried out in DMSO. The electrical conductivity of iodine doped PBIs were carried and the effect of iodine doping time on electrical conductivity was also studied.

2. Experimental

2.1. Materials

o-Phenylenediamine, 5-bromo-2-hydroxybenzaldehyde and 2-hydroxy-3-methoxy benzaldehyde were purchased from Sigma-Aldrich. Sodium bisulphite, potassium hydroxide,

CONTACT Athianna Muthusamy muthusrkv@gmail.com PG and Research Department of Chemistry, Sri Ramakrishna Mission Vidyalaya College of Arts and Science, Coimbatore, Tamil Nadu 641020, India.

Color versions of one or more of the figures in the article can be found online at www.tandfonline.com/lmsa.

sodium hypochlorite (4%,), hydrochloric acid and the solvents used were purchased from Merck and used as received.

2.2. Synthesis of monomer

The monomer BIBP was synthesized by condensing o-phenylenediamine with 5-bromo-2-hydroxybenzaldehyde. 5-bromo-2-hydroxybenzaldehyde in dimethyl formamide (DMF) was treated with sodium bisulphite at room temperature with constant stirring. The white solid bisulphite adduct formed was treated with equimolar quantity of o-phenylene diamine and heated to 80°C. The progress of the reaction was monitored with thin layer chromatography.[21] After completion of the reaction, the reaction mixture was cooled to room temperature and added into distilled water with vigorous stirring. The yellowish brown coloured solid formed was filtered, washed with hot water, dichloromethane and dried in vacuum oven. The other monomer BIMP was also synthesized by adopting the similar procedure. The monomers were obtained with good yield. (BIBP: 86% and BIMP: 80%). The syntheses of benzimidazoles are shown in Scheme 1.

BIBP: ^{1}HNMR (d6-DMSO): δ ppm 13.29 (s, 1H, Ar-OH and -NH), 7.02 (d, 1H, Ar-Ha), 7.48 (d, 1H, Ar-Hb), 7.29 (s, 1H, Ar-Hc), 8.29 (d, 1H, Ar-Hd), 7.70 (d, 1H, Ar-He). ^{13}CNMR (d6-DMSO): δ ppm, 157.62 (C7), 150.77 (C1), 141.06 (C10), 134.43 (C5), 133.77 (C3), 123.44 (C9), 120.11 (C6), 118.44 (C2), 115.25 (C8), 112.06 (C4). **BIMP**:^{1}HNMR (d6-DMSO): δ ppm 13.28 (s, 1H, Ar-OH, -NH), 3.89 (s, -OCH_3), 6.97 (d, 1H, Ar-Ha), 7.17 (d, 1H, Ar-Hb), 7.56 (d, 1H, Ar-Hc), 7.91 (d, 1H, Ar-Hd), 7.67 (d, 1H, Ar-He). ^{13}CNMR (d6-DMSO): δ ppm, 152.44 (C7), 149.40 (C1), 148.34 (C2), 139.54 (C10), 121.62 (C4), 120.26 (C9) 122.38 (C5), 116.16 (C6), 115.1 (C8), 110.7 (C3), 56.11 (−OCH_3).

2.3. Synthesis of polymer

The synthesized benzimidazoles were converted in to polybenzimidazoles by oxidative polycondensation method. A typical procedure for the oxidative polymerization of BIBP is as follows. An aqueous KOH solution of BIBP in 1:1 molar ratio was heated at 60°C with constant stirring. Then two molar quantities of NaOCl was added in drop wise and heated to 90°C.[22] After 24 hours, the contents were cooled to room temperature and neutralized with 4N HCl. The brown coloured solid polymer formed was filtered, washed with hot water and THF to remove the mineral salt and unreacted monomer respectively. The polymer of BIBP, poly-2-(1H benzo[d]imidazole-2-yl)-4-bromophenol (PBIBP) was dried in a vacuum oven at 80°C to constant weight. Poly-2-(1H benzo [d] imidazole-2-yl)-6-methoxyphenol (PBIMP) was also synthesized by adopting the similar procedure. The polymers were obtained with good yield. (PBIBP: 76% and PBIMP: 73%). The polymerization reactions are shown in Scheme 2.

PBIBP: ^{1}HNMR (d6-DMSO): δ ppm 10.60 (Terminal -OH), 13.24 (s, 1H, -NH), 6.97–8.14 (m, Ar-H). ^{13}CNMR (d6-DMSO): δ ppm, 157.51(C7), 150.84(C1), 141.02(C10), 133.77 (C5), 132.1(C3), 124.96(C9), 120.56 (C6), 115.21(C8), 118.56 (C2), 112.82 (C4), 147.73, 145.61, 144.09 (C-O-C), 130.43, 129.36 (C-C). **PBIMP**:^{1}HNMR (d6-DMSO): δ ppm 9.67 (Terminal -OH), 13.12 (s, 1H, -NH), 3.91(s, -OCH_3), 7.05–7.86(m, Ar-H). ^{13}CNMR (d6-DMSO): δ ppm, 150.01(C7), 148.94(C1), 147.28(C2), 139.51(C10), 121.17(C4), 120.38(C9) 124.06 (C5), 116.26 (C6), 114.76 (C8), 110.07 (C3), 57.00 (OCH_3), 146.67 (C-O-C), 131.94, 126.03, 119.45(C-C).

2.4. Characterization techniques

FT-IR spectra were recorded in KBr pellet in the region 400–4000 cm^{-1} using Perkin Elmer FT-IR 8000 spectrophotometer. NMR spectra were recorded with Bruker AV400 MHZ spectrometer by using DMSO-d_6 as a solvent. UV-visible spectra were recorded in DMSO solution using Systronics double beam UV-visible spectrophotometer 2202 in the range 200–800 nm. The emission spectra of monomers and polymers were recorded on a JobinYvon Horiba Fluoromax-3 spectrofluorometer in DMSO solution. The quantum theoretical calculations using DFT, at B3LYP/6-31(d, p) basis in the Gaussian 09 package were carried out for monomers. The electrical conductivity of the polymers was measured with Keithley 6517B Electrometer using four-point probe technique. Iodine doping was carried out by exposing the polymer pellet with iodine vapour at atmospheric pressure in a desiccator at room temperature. The charge density of monomer was calculated by Huckel calculation method. The dielectric studies of the polymers were carried out using Hioki 3532–50 LCR meter at various temperatures in the frequency range of 50 Hz to 5 MHz. TG measurements were made in HITACHI 7300PC thermal analyser between 30°C and 500°C (in N_2; rate, 10°C/min).

3. Results and discussion

3.1. Solubility

The solubility of the monomers and polymers in assorted solvents was checked by dissolving 0.1 g of the sample in 1 ml of

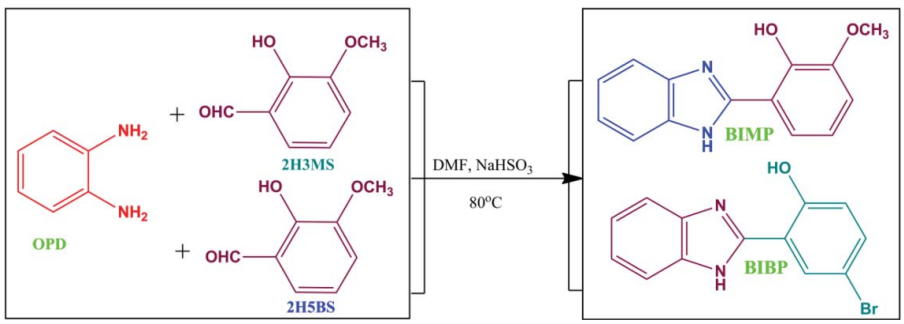

Scheme 1. Synthesis of monomer.

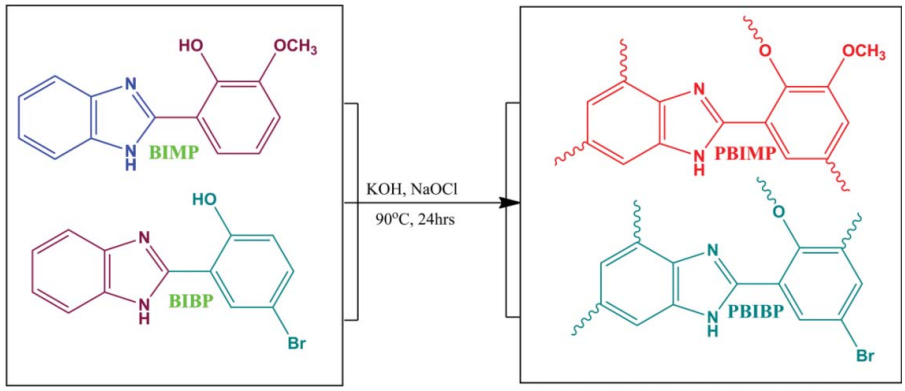

Scheme 2. Synthesis of polymer.

solvent. The monomers and polymers are soluble in polar solvents methanol, DMSO, DMF and DMAC, sparingly soluble in chloroform, ethanol and insoluble in non-polar solvents. All though the polymers are having polar terminal phenolic group the solubility of polymers is less than the monomers due to the existence cross links in polymer backbone.[23] The molecular weight of polymer PBIBP and PBIMP was determined by Gel permeation chromatography. The number average molecular weight (Mn), weight average molecular weight (Mw) and Dispersity of polymers were calculated from polystyrene standard calibration curve. The Mn, Mw and Dispersity values of PBIBP and PBIMP are found to be 1950, 2021 g mol^{-1}, 1.03 and 2150, 2950, 1.37 respectively. The Dispersity value shows that the PBIBP more homogeneous than the PBIBP.[21]

3.2. Spectral characterization

The FT-IR spectra of benzimidazole monomers and polymers are shown in SF. 1 and the spectral data are given in Table 1. When FT-IR spectra of monomers are compared with the respective polymers, polymer showed little depth and wide peaks as the π conjugation in the polymer chain increases. The sharp peaks between 3372 and 3335 cm^{-1} were caused by –NH stretching frequency of monomers and polymers. The range between 1624 and 1585 cm^{-1} ascribed to —C=N-stretching of monomers and polymers. The characteristic peak of phenolic —OH stretching of monomers appear at around 3480 cm^{-1}. The peaks in the range of 3000-1800 $cm^{-1}$is attributed to the hydrogen bonding association of monomers.[24] In the FT-IR spectra of polybenzimidazoles, the peak appeared in the range of 3491–3460 cm^{-1} which would be attributed to the terminal —OH groups. The phenolic C—O—C stretching vibrations in polymer appear in the range of 1128–1138 cm^{-1}.This is an evident that the polymerization has taken place through the C—O—C coupling.[25] Besides, an additional peak shown by the polymers at 841 cm^{-1} is due to the stretching of the C—C linkage of phenylene units formed through polycondensation.[26] These spectral results confirm that the polycondensation has taken place through both C-C and C-O-C coupling. The peaks in the range of 1444–1482 cm^{-1} were owes to aromatic —C=C— stretching frequencies of monomers and polymers. The peaks at around 3055 cm^{-1} attributed to aromatic —CH stretching frequency of monomers and polymers.

Table 1. FT-IR spectral data of monomers and polymers.

	Wave number (cm^{-1})						
Compound	—OH	—C=N—	—NH	—C=C—	C—O—C	Ar—CH	Ar—C—Br
BIBP	3485	1585	3336	1444	—	3066	544
PBIBP	3491	1621	3367	1482	1138	3051	558
BIMP	3494	1621	3335	1462	—	3072	—
PBIMP	3460	1624	3372	1460	1128	3055	—

The ^{1}H and ^{13}C NMR spectra of monomers and polymers are shown in Figure 1 and 2. ^{1}H and ^{13}C NMR spectral data of monomers and polymers are given in experimental part. Imidazole -NH and -OH protons show only a broad single band in the spectra of BIBP and BIMP and appearing 13.29, 13.28 ppm respectively. The – OH protons of monomers are involved in strong intramolecular hydrogen bonding with the imine nitrogen (=N—) which leads to stronger deshielding and are merged with —NH protons.[27] Whereas, in polymers the phenolic –OH groups are involved in polymerization and are not available for involving in hydrogen bonding with imine. The terminal phenolic–OH protons of polymers are unable to form hydrogen bonding with imine and thereby the protons are not deshielded and appearing at 10.60 and 9.67 ppm respectively for PBIBP and PBIMP. Further there is no significant change in chemical shift values of imidazole —NH proton (PBIMP; 13.12 and PBIBP; 13.24 ppm) when compared with monomer. The aromatic protons of monomer BIBP (Ha) and BIMP (Hb) were appeared at 7.02 and 7.17 ppm respectively. The —OCH_3 group of BIMP and PBIMP showed sharp signals at 3.89 and 3.91 ppm respectively. The peaks of Ha (BIBP) and Hb (BIMP) protons of monomers are slightly shifted to deshielded region in polymers as these protons are involved polycondensation. The ^{1}H NMR spectra of monomers give very sharp peaks but there is increase in number and enlargement of the peaks observed after polycondensation. This enlargement maybe due to the formation of repeating units in polymer with different chemical environments through C—C & C—O—C couplings.[28,29] As the polymerization involving aromatic protons with these two types of couplings changing the chemical environment of neighboring protons which leads to the appearance some new peaks in the spectra of polymers.[30]

The^{13}C NMR spectra of monomers and polymers are differing in their number of peaks and chemical shift values. The C4, C8, C9 and C2, C8, C9 carbons of BIMP and BIBP resonate at 121.62, 115.1, 120 .26 and 118.44, 115.25, 123.44 ppm respectively. The shifting of chemical shift values of these carbons in PBIBP to 121.17, 114.76, 120.28 and PBIMP to118.56, 115.21,

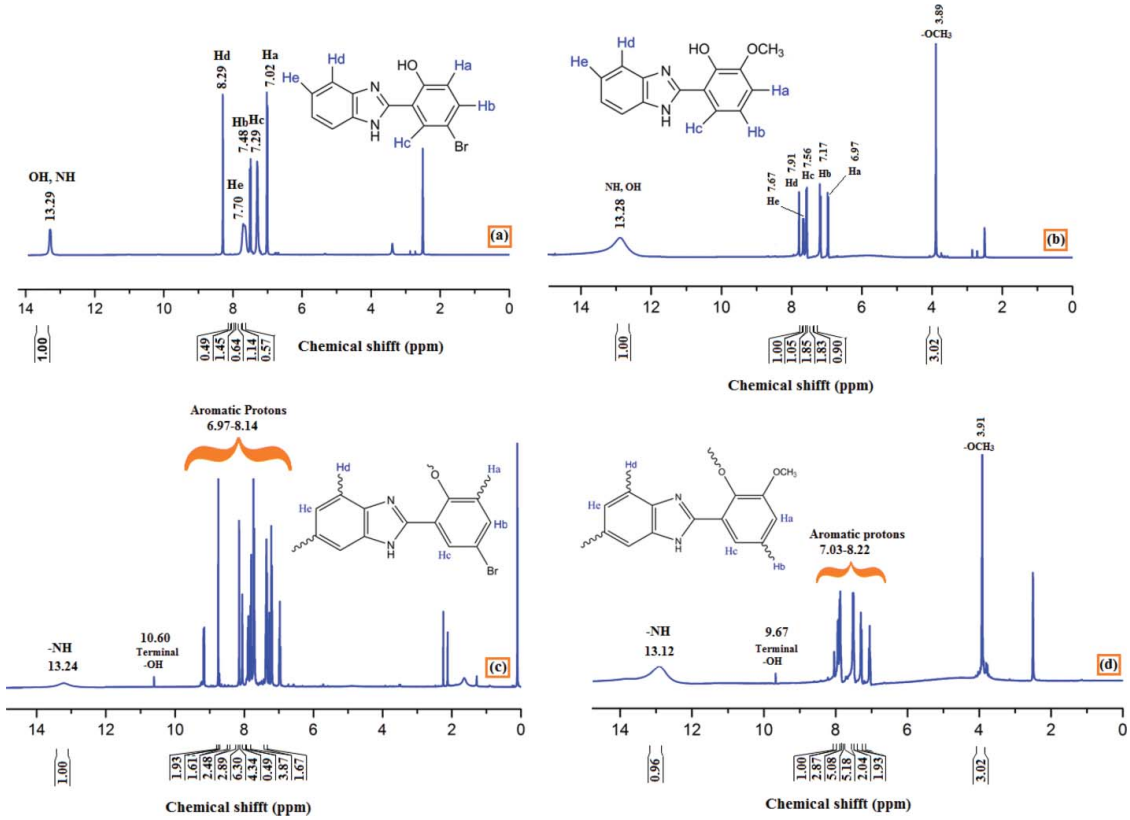

Figure 1. [1]H NMR spectra of (a)BIBP, (b) BIMP, (c)PBIBP and (d) PBIMP.

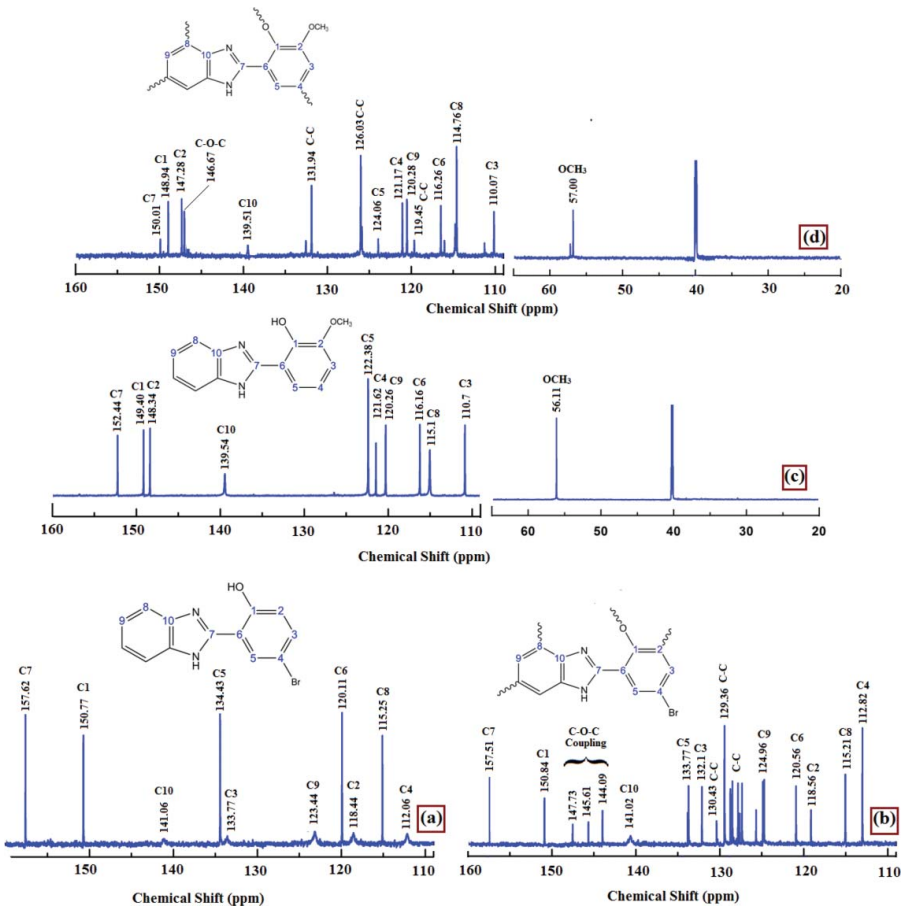

Figure 2. [13]C NMR spectra of (a)BIBP, (b) PBIBP, (c) BIMP and (d) PBIMP.

124.96 ppm indicating that the oxidative polymerization proceeds with these carbons.[31] The appearance of two sets of new peaks in spectra of PBIBP and PBIMP may be due to the carbons of C-O-C and C-C linkages. The two sets of values for each linkage indicating the two possibilities of coupling for C—O—C and C—C coupling.

3.3. Optical properties

UV-visible spectra of the benzimidazole monomers and polymers were recorded in DMSO (0.03 g/L) solution and are shown in SF.2. The $\pi \rightarrow \pi^*$ and $n \rightarrow \pi^*$ transitions of the aromatic ring and imidazole moiety of monomers observed at 218, 243, 302 and 335 nm. The distinctive absorption band of azole chromophore appears at around 330 nm for both monomers and polymers. Moreover, the usual $\pi \rightarrow \pi^*$ and $n \rightarrow \pi^*$ transitions of imidazole and benzene moiety at around 218 and 243 nm respectively are also shown by polymers.

The relative intensity of polymers is low when compared with monomers due to the destruction of planarity of the molecules during polymerization.[32] This is reflected in the band gap values also. The optical band gap (E_g) is obtained from the equation $E_g = 1242/\lambda_{onset}$.[33] Where λ_{onset} is, the onset wavelength obtained from intersection of two tangents on the absorption edges. The band gap values of monomers are greater than polymer, due to the polyconjugated structure.[34] The optical band gap values of monomers and polymers are given in Table 2.

The fluorescence spectra of the monomers and polymers were recorded in DMSO solution at 100 mg/L concentration and slide width is 5 nm for excitation wavelength for monomers and polymers. The fluorescence emission spectra of monomers and polymers are shown in Figure 3. The fluorescence emission of monomers and polymers appears in the blue region of the spectrum. The monomer emissions are appearing at 479 for BIBP and 472 for BIMP. In general the intensity of fluorescence emission is influenced by the nature of the substituent present.[35] The intensity of fluorescence emission of BIMP and PBIMP are greater than BIBP and PBIBP due to the presence of electron donating $-OCH_3$ group in the former and electron withdrawing –I bromine in the later.[36]

3.4. Theoretical studies

The quantum theoretical calculations using DFT, at B3LYP/6–31(d, p) basis in the Gaussian 09 package were carried out for monomers. Based on the optimized geometries the energy and electronic distribution of molecular frontier orbital's were calculated in vacuum phase. In BIBP and BIMP monomers, the highest occupied molecular orbital is concentrated in the phenyl rings.

This corresponds to the calculations of electron density, which indicate that this region has the highest density of negative charge. Lowest unoccupied molecular orbital's are localized on imidazole and phenolic rings of the molecule. The simulation results including the optimized molecular configuration, energy levels and electron distribution of the HOMO and LUMO of BIMP and BIBP monomers are shown in SF.3. The HOMO electrons are averagely distributed on the whole molecule's backbone, but LUMO electrons are located in phenolic and imidazole part of monomers. The calculated energy levels of HOMO and LUMO are −5.41, −5.54 and −1.19, −1.52 eV for BIMP and BIBP respectively. The energy gap was calculated from HOMO and LUMO for BIMP and BIBP are 4.21 and 4.09 eV respectively. The theoretically calculated energy gap values are slightly far from the experimentally calculated values from UV-visible spectra (Table 2). The differences may be related to various effects of conformations of benzimidazole monomers in vacuum, solid and solutions.

Table 2. Optical data of monomers and polyners.

Compound	Absorption			Emission		
	$\lambda_{max\ (nm)}$ [a]	λ_{onset} [b]	Eg[c](ev)	λ_{Ex} [d]	λ_{Em} [e]	I_{Em} [f]
BIBP	217, 243, 337	381	3.25	345	479	109
BIMP	218, 243, 336	354	3.41	320	472	578
PBIBP	216, 243, 325	375	3.31	340	463	400
PBIMP	217, 243, 335	395	3.13	330	472	780

[a]Absorption maximum; [b]Absorption edges by intersection of two tangents; [c]Band gap values; [d]Excitation wavelength for emission; [e]Maximum emission wavelength; [f]Maximum emission intensity

3.5. Conductivity measurements

Electrical conductivities of the polymers and its variation on doping time from 0–144 hrs with p-type oxidative dopant iodine was determined by using four probes connected with Keithley 6517B electrometer. The increase in conductivity is due to the formation of charge transfer (CT) complex by iodine with imidazole nitrogen atom and aromatic π-electron cloud of the polymer chain. The increase in conductivity with iodine vapour exposure time is shown in Figure 4. The maximal conductivity values of polymers are found to be 1.50×10^{-7} for PBIBP and $1.35 \times 10^{-7} Scm^{-1}$for PBIMP. The higher maximal conductivity values for PBIBP when compared with PBIMP may be due to high electron density on imidazole nitrogen, which leads to greater doping of iodine.[37]

The charge density on imidazole nitrogen was calculated by Huckel method and is given in SF.4. The charge on imidazole nitrogen of BIBP (0.365) is greater than the BIMP (0.364) and there is a greater tendency of coordination with iodine in BIBP. The conductivity of polymers slowly increases with increasing doping time and tends to level off after 144 hours. The polymers on doping with iodine for 144 hours the conductivity of polymers PBIBP and PBIMP are increased about 10^4 order of magnitude respectively. The expected doping mechanism is connected with the removal electrons from HOMO of PBIBP leaving positive holes behind and I_3^- counter ions formation. Positive polaron formation in PBIBP is connected with transformation of conjugated benzenoid chain fragments into quinonoid one.[38]

$$(PBIBP) + 3I_2 \rightarrow 2I_3^- + (PBIBP)^+$$

The doping of iodine increases the conductivity of polymers and thereby these can be used for the application of gas sensor against electron acceptor gases.[39–42]

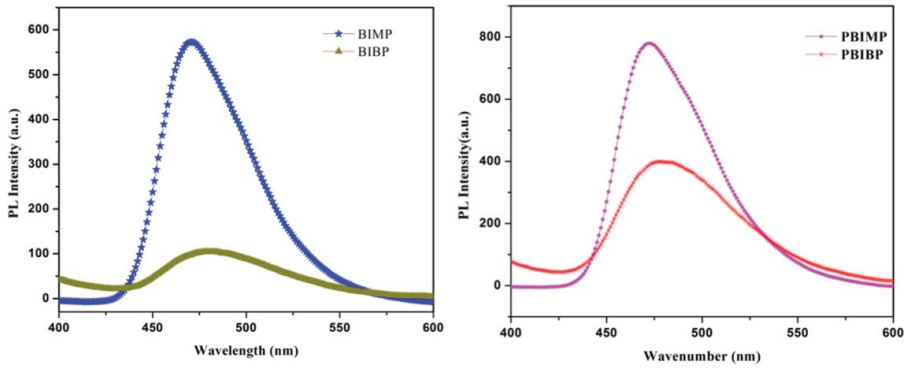

Figure 3. Fluorescence emission spectrum of monomers and polymers.

3.6. Thermal properties

The thermal stability of the synthesized polymers was studied with thermo gravimetric analysis in nitrogen atmosphere. The TG traces of the polymer are given in Figure 5. The thermal data, the temperature corresponding to 10, 30 and 50% weight loss and char residue are given in Table 3. The initial weight loss up to 100°C may be due to the presence of occluded moisture in the polymers.[43] The initial degradation of polymers starts at 166°C for PBIBP and 171°C for PBIMP. On comparing the initial degradation temperature, 10, 30 and 50% weight loss, thermal stability of PBIBP is greater than PBIMP. Thermal stability polymer PBIBP is greater than PBIMP due to the bromine substituent present in former and thermally weakly bonded $-OCH_3$ substituent present in later.[44] These results suggest that the polymerization proceed dominantly via C—C coupling which results in high carbine residue. Further it confirms that the weaker C—O—C coupling has taken place relatively less extent during the polymerization.[45] The polymers have good thermal stability even at 500°C, due to long conjugation and higher aromatic content in the polymer skeleton. The high carbon residue suggests that the polymerization proceeds predominantly with C-C than C-O-C coupling.[46] The obtained DSC curve of polymers is shown in SF.5 and 6. There is no glass transition temperature (T_g) for synthesized polymers and melting point (T_m) of PBIB and PBIMP obtained at 97.80, 197.70& 256.13°C and 103.31 & 248.72°C respectively.

3.7. Dielectric properties

The variation of dielectric properties of synthesized polymers was characterized as a function of frequency and temperature. The dependence of dielectric constant and loss of polymers are shown in Figure 6. The dielectric constant of the polymer was calculated using the formula.[47]

$$\varepsilon_r = Cd/\varepsilon_0 A$$

Where, C is the capacitance and d is the pellet thickness, A is the cross sectional area of the pellet and ε_0 is the free space permittivity of the pellet. The dielectric constant of polybenzimidazoles increases with decrease in frequency and attained a constant value after a certain frequency. At high frequency polymer molecules do not have enough time to get polarized and thereby dielectric constant is less. Whereas, at low frequency polymer molecules are having enough time to get polarized and recorded high dielectric constant.[34]

The dielectric constant is very high at a low frequency of 50 Hz at 120°C (Figure 7) as the intermolecular forces between polymer chains are minimized and enhanced thermal agitation of polymer chains. At low temperature the segmental motion of the polymer chains are freezed and thereby dielectric constant decreased. The variation of dielectric constant can also be explained with help of variation dipole moment with temperature. At low

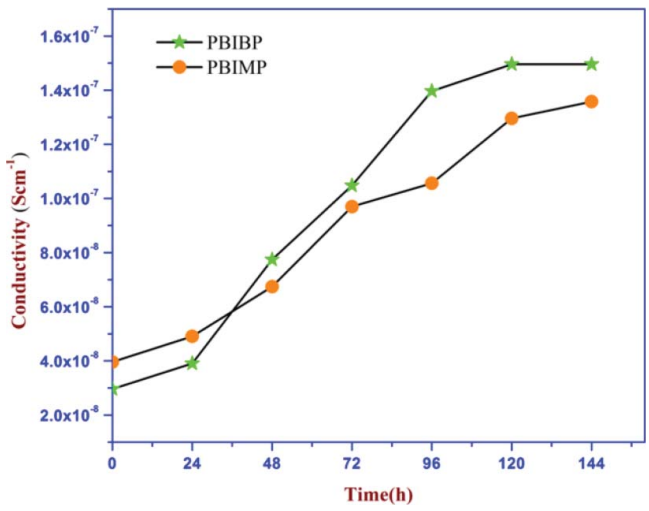

Figure 4. Electrical conductivity of iodine doped and undoped polybenzimidazoles.

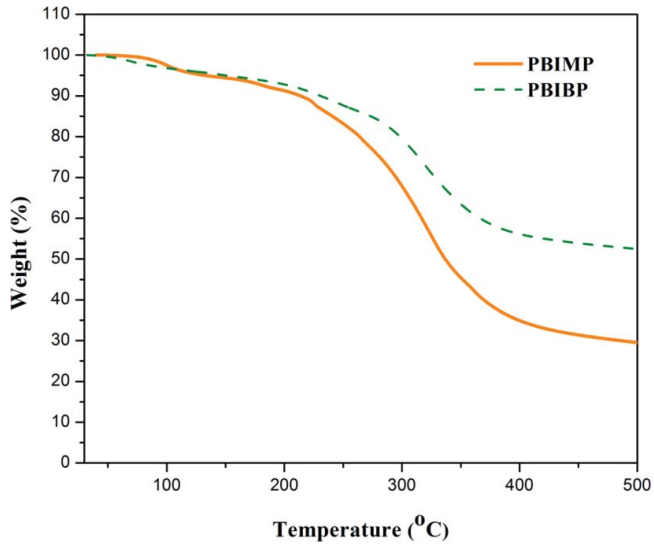

Figure 5. TG Curve of PBIBP and PBIMP.

Table 3. Thermal data of polymers.

	TGA					DSC
		% Weight loss			% Char Residue at	
Compound	T_{on}	10	30	50	500°C	Tm
PBIBP	166	231	326	—	52	97.80 & 197.70
PBIMP	171	215	296	335	30	103.31 & 248.72

temperature with higher frequency dielectric constant of PBIMP and PBIBP are decreased due to low space charge polarization. Whereas, at high temperature with lower frequency dielectric constant of polymers are increased as space charge polarization dominates.[48] The dielectric constants of polymers at 120°C (50 Hz) are 63.17 (PBIMP) and 45.53 (PBIBP). The higher dielectric constant of PBIMP polymer maybe due to its greater dipole moment than the PBIBP. The dipole moment has been confirmed theoretically using DFT, at B3LYP/6–31(d, p) basis in the Gaussian 09 package. The dipole moment of monomers is 4.30 and 3.72D for BIMP and BIBP respectively.[49] Therefore, PBIMP with greater dielectric constant can be used to make passive component like capacitors, resistors etc.[50] The difference in dielectric loss at different temperatures with increase in frequency is shown in Figure 6 (b, d). The dielectric loss of polymers is due to three distinct effects such as, space charge polarization, DC resistivity and orientation polarization. The high value of dielectric loss at low frequencies and low at high frequencies are mainly due to DC conduction and space charge polarization.[51] The frequency increases exponentially with decrease in dielectric loss and it can be recognizing from the plot. The dielectric loss decreases with increasing frequency is observed and promise with Debye's type relaxation process.[52] In the high

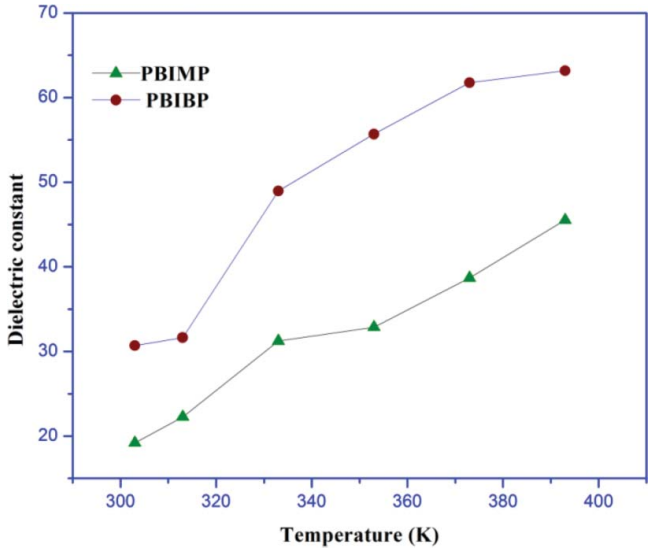

Figure 7. Dielectric constant of polymers with different temperature at 50 Hz.

frequency region the low dielectric loss obtained suggest that the synthesized polymers can be used for capacitors, radiation detectors, resistors, thermionic valves and electro-optical device applications.[53]

3.7.1. AC conductivity

$$\sigma_{ac} = 2\pi f \, (\tan\delta) \, \varepsilon' \varepsilon_o$$

Where, f is the frequency of applied voltage, ε_o is permittivity of free space and tanδ is dielectric loss. The frequency and temperature dependent AC conductivity plot of polymers are

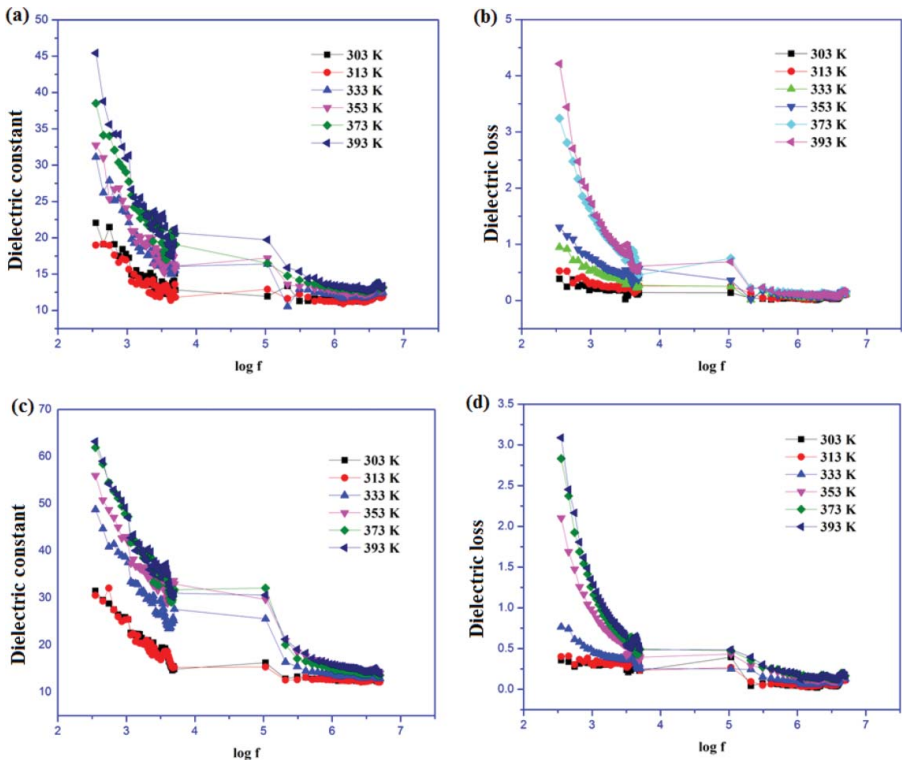

Figure 6. Dielectric constant (a, c) and dielectric loss (b, d) of polymers PBIBP and PBIMP with temperature.

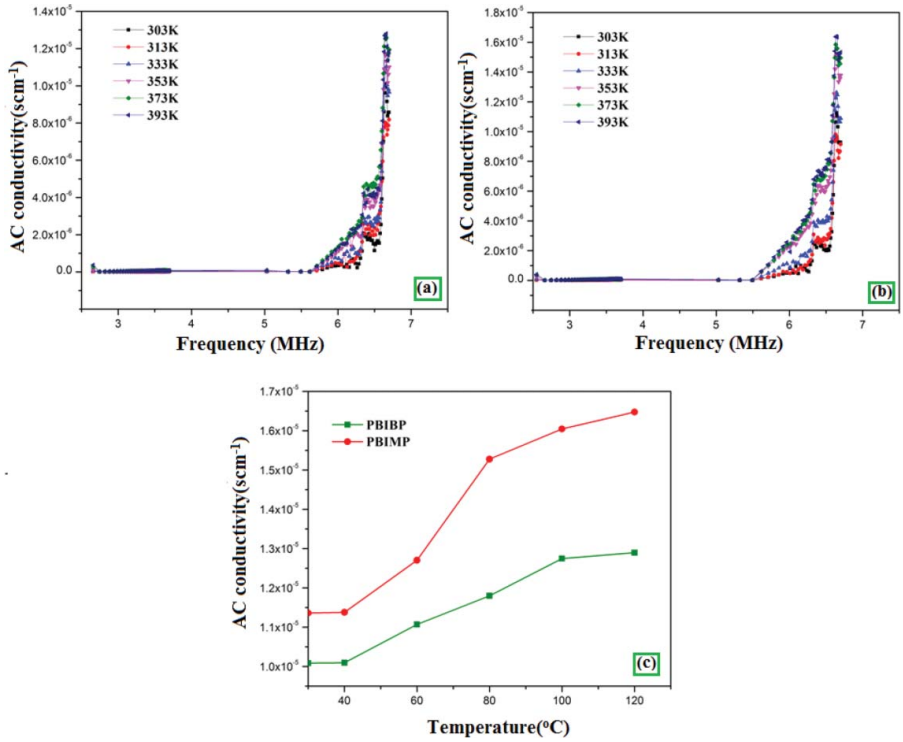

Figure 8. Frequency dependent Ac conductivity of polymer (a) PBIBP (b) PBIMP and Temperature dependent Ac conductivity of PBIBP and PBIMP(c).

shown in Figure 8 (a, b). The conduction mechanism of polymers can be explained on the basis of hopping mechanism. The polymers show AC conductivity only after 5 MHz indicating the formation of excess charge carriers (polaron and bipolaron) at higher frequencies. The conductivity values of polymers depend on microscopic and macroscopic conductivities. The microscopic conductivity depends upon the conjugation length or chain length etc, whereas the macroscopic conductivity depends on the inhomogeneities in the polymers, compactness of pellets and orientation of micro particles.[54] Since polymers are synthesized by oxidative polycondensation the chain length of polymers are increased by C-O-C and C-C linkages. So the microscopic conductivities of both the polymers are almost equal but the physical (macroscopic) properties may significantly vary due to the pellet compactness and molecular orientations leading to the increase conductivity.

The temperature dependence of AC conductivity of polymers is studied in the range of 303–393 K for different frequencies for the polymers. The variation of AC conductivity with temperature for polymers is shown in Figure 8 (c, d). The AC conductivity of polymers (at 120°C) found to be 1.6504×10^{-5} for PBIMP and 1.2915×10^{-5} $Scm^{-1}$for PBIBP. The AC conductivity polymer increases with increase of temperature, due to the increase in coefficient of thermal conductivity. In general in ionic and solid compounds the heat transfer is due to phonons. Therefore the value of coefficient thermal conductivity for these materials is low. In polymers heat transfer occurs by molecular rotation, vibration and transition and, hence the value of coefficient of thermal conductivity is less at low temperature. This can be attributed to the less amount of phonons are available for interactions and this leads to an increase thermal boundary resistance. Whereas at high temperature the phonons are excited, the probability of interaction among the phonons through the Umklapp processes increases and this leads to the increase thermal conductivity of polymers.[55]

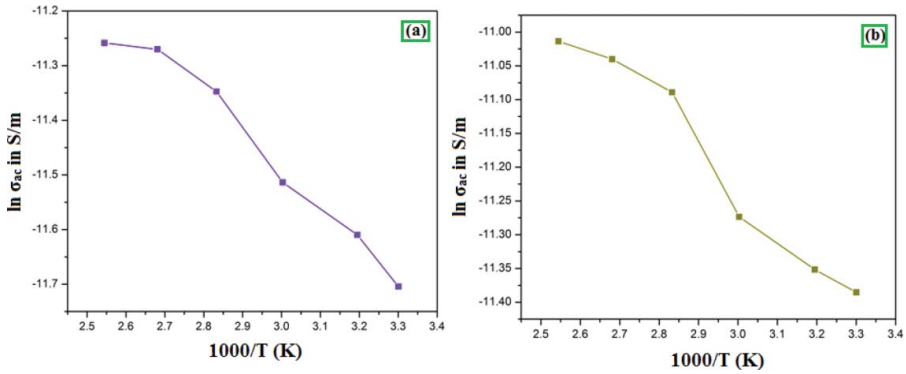

Figure 9. Variation of $\ln\sigma_{ac}$ in S/m with 1000/T (K) of polymer (a) PBIBP and (b) PBIMP.

3.7.2. Activation energy

The activation energy of polymers was calculated from the slope of Arrhenius plot obtained from the Arrhenius equation.

$$\sigma_{ac} = \sigma_0 \, exp\left(\frac{-E_\sigma}{KT}\right)$$

Where σ_0 is a constant, E_σ is the activation energy, K is Boltzmann's constant and T is the absolute temperature. Therefore, the polymer exhibits Arrhenius type of conductivity behavior in the temperature range of investigation. The Arrhenius plot of σ_{ac} versus 1000/T is shown in Figure 9. The activation energy of polymer PBIBP and PBIMP calculated from the plot and is found to be 0.51 and 0.33 eV. Activation energy of polymer PBIMP is low compared to the PBIBP. This may be attributed to the low conductivity and low mobility carriers in the polymer PBIMP.[56]

4. Conclusion

Two polybenzimidazoles were effectively synthesized by oxidative polymerization method using NaOCl as an oxidant in an aqueous alkaline medium. The polymers were characterized by UV-visible, FT-IR, NMR analyses. FT-IR and NMR spectral results indicate that polymerization of the monomer by OP has taken place through C-C and C-O-C couplings. The polymers are having high fluorescent emission (blue region), so it can be used in the preparation of the alternative blue light emitting diodes and as optical sensors. The synthesized polymers have low band gaps than the monomer due to the polyconjugated structure. Iodine vapour doped polymer PBIBP gave the maximum electrical conductivity of 10^{-6} Scm^{-1} due formation of a charge transfer complex with iodine and also the presence of electron rich imidazole moiety. The increase in conductivity with iodine shows that the polymers are best candidates for gas sensing applications against electron acceptor gases. A high char residue in TG analysis suggests that the polymerization proceeded predominantly via C-C coupling. The dielectric constant of PBIMP is greater than the PBIBP at 393K is due to the space charge polarization. So the PBIMP can be used to make reactive component like capacitors and resistors. Activation energy PBIBP and PBIMP for the conduction process calculated from the plot and is found to be 0.51 and 0.33 eV.

References

[1] Rahimabady, M.; Mirshekarloo, M. S.; Yao, K.; Lu, L. *Phys. Chem. Chem. Phys.* **2013**, *15*, 16242–16248.
[2] Shen, Y.; Liang, G.; Yua, L.; Qiang, Z.; Gu, A. *J. Alloys. Compd.* **2014**, *602*, 16–25.
[3] Zhang, Y.; Ke, S.; Huang, H.; Zhao, L.; Yu, L.; Chan, H. *Appl. Phys. Lett.* **2008**, *92*, 52910.
[4] Yu, L.; Zhang, Y. H.; Shang, J.; Ke, S. M.; Tong, W. S.; Shen, B.; Huang, H. T. *J. Electron. Mater.* **2012**, *412*, 439–2446.
[5] Jiang, L.; Liu, J.; Wu, D.; Li, H.; Jin, R. *Thin Solid Films.* **2006**, *510*, 241–246.
[6] Min, C. K.; Wu, T. B.; Yang, W. T.; Chen, C. L. *Compos. Sci. Technol.* **2008**, *68*, 1570–1578.
[7] Zhang, Y.; Yu, L.; Su, Q.; Zheng, H.; Huang, H.; Chan, H. L. M. *J. Mater. Sci.* **2012**, *47*, 1958–1963.
[8] Wang, C.; Zhao, X.; Jiang, Li, G. *J. Colloid. Polym. Sci.* **2011**, *289*, 1617–1624.
[9] Yu, W.; Fu, J.; Dong, X.; Chen, L.; Shi, L. *Compos. Sci. Technol.* **2014**, *92*, 112–119.
[10] Zhou, T.; Zha, J. W.; Cui, R. Y.; Fan, B. H.; Yuan, J. K.; Dang, Z. M. *ACS. Appl. Mater. Interfaces.* **2011**, *3*, 2184–2188.
[11] Dang, Z. M.; Lin, Y. H.; Nan, C. W. *Adv. Mater.* **2003**, *15*, 1625–1629.
[12] Shen, Y.; Lin, Y. H.; Nan, C. W. *Adv. Funct. Mater.* **2007**, *17*, 2405–2410.
[13] Dang, Z. M.; Lin, Y. Q.; Xu, H. P.; Shi, C. Y.; Li, S. T.; Bai, J. B. *Adv. Funct Mater.* **2008**, *18*, 1509–1517.
[14] Xiao, M.; Sun, L. Y.; Liu, J. J.; Li, Y.; Gong, K. C. *Polymer.* **2002**, *43*, 2245–2248.
[15] Yu, L.; Zhang, Y.; Tong, W.; Shang, J.; Shen, B.; Lv, F.; Chu, P. K. *RSC. Adv.* **2012**, *2*, 8793–8796.
[16] Maity, S.; Jana, T. *Macromolecules* **2013**, *46*, 6814–6823.
[17] Singha, S.; Jana, T. *Polymer.* **2014**, *55*, 594–601.
[18] Maity, S.; Jana, T. *ACS Appl. Mater. Interfaces.* **2014**, *6*, 6851–6864.
[19] Singha, S.; Jana, T. *ACS Appl. Mater. Interfaces.* **2014**, *6*, 21286–21296.
[20] Maity, S.; Sannigrahi, A.; Ghosh, S.; Jana, T. *Eur. Polym. J.* **2013**, *49*, 2280–2292.
[21] Anand, S.; Muthusamy, A.; Dineshkumar, S.; Chandrasekaran, J. *J. Mole. Struct.* **2017**, *1147*, 351–363.
[22] Dineshkumar, S.; Muthusamy, A. *Polym. Plast. Technol. Eng.* **2016**, *55*, 368–378.
[23] Bilici, A.; Kaya, I.; Yıldırım, M. *Eur. Polym. J.* **2011**, *47*, 1005–1017.
[24] Kaya, I.; Etiner, A.; Mehmet Sac, A. K. *J. Macromol. Sci. Part A Pure Appl. Chem.* **2007**, *44*, 463–468.
[25] Dogan, F.; Kaya, I.; Temizkan, K. *Eur. Polym. J.* **2015**, *66*, 397–406.
[26] Premachandran, R. S.; Banerjee, S.; Wu, X. K.; John, V. T.; Mcpherson, G.; Akkara, J.; Ayyagari, M.; Kaplan, D. *Macromolecules.* **1996**, *29*, 6452–6460.
[27] Tavman1, A.; Ikiz, S.; Funda Bagcigil, A.; Yakut Ozgur,, N.; Seyyal, A. K. *J. Serb Chem. Soc.* **2009**, *74*, 537–548.
[28] Dilek, D.; Dogan, F.; Bilici, A.; kaya, I. *Thermochim. Acta.* **2011**, *518*, 72–81.
[29] Kumbul, A.; Gokturk, E.; Sahmetliogl, E. *J. Polym. Res.* **2016**, *23*, 52.
[30] Kaya, I.; Kartal, E.; Şenol, D. *Des. Monomers. Polym.* **2015**, *18*, 524–535.
[31] Kaya, I.; ıtakoglu, N.; Kolcu, F. *Polym. Bull.* **2016**, DOI: 10.1007/s00289-016-1780-6.
[32] Mohan, J. *organic chemistry principles and application*, 2nd ed.; Narosa: India, **2007**.
[33] Avcı, A.; Kamacı, M.; Kaya, I.; Yıldırım, M. *Mater. Chem. Phys.* **2015**, *163*, 301–310.
[34] Dineshkumar, S.; Muthusamy, A. *Des. Monomers. Polym.* **2016**, *20*, 234–249.
[35] Fan, C.; Pu, S.; Liu, G.; Yang, T. *J. Photochem. Photobiol. A.* **2008**, *197*, 415–425.
[36] Chen, C. T.; Chiang, C. L.; Lin, Y. C.; Chan, L. H.; Huang, C. H.; Tsai, Z. W.; Chen, C. T. *Org.Lett.* **2003**, *5*, 1261–1264.
[37] Dineshkumar, S.; Muthusamy, A. *J. Mole. Struct.* **2017**, *1128*, 730–740.
[38] Hajduk, B.; Weszka, J.; Jarząbek, B.; Jurusik, J.; Domanski, M. *J Achiev Mat and Manu Eng.* **2007**, *24*, 67–70.
[39] Diaz, F. R.; Moreno, J.; Tagle, L. H.; East, G. A.; Radic, D. *Synth. Met.* **1999**, *100*, 187–193.
[40] Kolcu, F.; Kaya, I. *J. Macromol. Sci. Part A. Pure. Appl. Chem.* **2016**, *53*, 438–451.
[41] Bilici, A.; Kaya, I.; Yıldırım, M.; Dogan, F. *J. Mol. Catal. B: Enzym.* **2010**, *64*, 89–95.
[42] Bilici, A.; Dogan, F.; Yıldırım, M.; Kaya, I. *Materials Chemistry and Physics.* **2013**, *140*, 66–74.
[43] Avcı, A.; Kaya, I. *Tetrahedron. Lett.* **2015**, *56*, 1820–1824.

[44] Dineshkumar, S.; Muthusamy, A.; Chitra, P.; Anand, S. *J. Adhes. Sci and Tech.* **2015**, *29*, 2605–2621.
[45] Şenol, D.; Kaya, I. *J Saudi Chem Soc.* **2015**, DOI: 10.1016/j.jscs.2015.05.006.
[46] Kaya, I.; Bilici, A.; Tezel, R. N.; Temizkan, K.; Dogan, F. *J. Macromol. Sci. Part A Pure Appl. Chem.* **2017**, *54*, 243–248.
[47] Ahmad, Z. *Polymer Dielectric Materials, Intech.* **2012**, https://doi.org/10.5772/50638.
[48] Khurmi, R. S.; Sedha, R. S. *Materials science*. S.Chand: India, **2011**.
[49] Bock, E.; Wasylishen, R.; Bernard, Gabour, E. *Chemis cher Informations dienst* **1973**, *4*, 36.
[50] Singh, R.; Ulrich, R. K. *Physicochemical Properties of Water-Soluble Contrast Media, The electrochemical society, Interface* **1999**, *8*, 26–30.
[51] Soares, B. G.; Leyva, M. E.; Barra, G. M.; Khastgir, D. *Eur Polym., J* **2006**, *42*, 676–686.
[52] Anand, S.; Muthusamy, A. *J. Mole. Struct.* **2017**, *1148*, 254–265.
[53] Arjunan, S.; Bhaskaran, A.; Mohan Kumar, R.; Mohan, R.; Jayavel, R. *Mater. Manuf Process.* **2012**, *27*, 49–52.
[54] Vishnuvardhan, T. K.; Kulkarni, V. R.; Basavaraja, C.; Raghavendra, S. C. *Bull. Mater. Sci.* **2006**, *29*, 77–83.
[55] Choy, C. L. *Polymer* **1977**, *18*, 984–1004.
[56] Hashima, M.; Alimuddin, S.; Kumar, Shirsath, S. E.; Mohammed, E. M.; Chung, H.; Kumar, R. *Physica B.* **2012**, *407*, 4097–4103.